HHS Public Access

Author manuscript

Curr Opin Chem Biol. Author manuscript; available in PMC 2019 May 04.

Published in final edited form as:

Curr Opin Chem Biol. 2018 August ; 45: 131–138. doi:10.1016/j.cbpa.2018.04.014.

Magnetic Particle Imaging for Radiation-Free, Sensitive and High-Contrast Vascular Imaging and Cell Tracking

Xinyi Y. Zhou[1,+,2], **Zhi Wei Tay**[1,2], **Prashant Chandrasekharan**[1], **Elaine Y. Yu**[1,2,*], **Daniel W. Hensley**[1,2,*], **Ryan Orendorff**[1,2,*], **Kenneth E. Jeffris**[1], **David Mai**[1], **Bo Zheng**[1], **Patrick W. Goodwill**[3], and **Steven M. Conolly**[1,4]

[1]Department of Bioengineering, University of California Berkeley, Berkeley CA 94720, United States

[2]UC Berkeley - UCSF Graduate Program in Bioengineering

[3]Magnetic Insight, Inc., Alameda, California 94501, United States

[4]Department of Electrical Engineering and Computer Sciences, University of California Berkeley, Berkeley CA 94720, United States

Abstract

Magnetic particle imaging (MPI) is an emerging ionizing radiation-free biomedical tracer imaging technique that directly images the intense magnetization of superparamagnetic iron oxide nanoparticles (SPIOs). MPI offers ideal image contrast because MPI shows zero signal from background tissues. Moreover, there is zero attenuation of the signal with depth in tissue, allowing for imaging deep inside the body quantitatively at any location. Recent work has demonstrated the potential of MPI for robust, sensitive vascular imaging and cell tracking with high contrast and dose-limited sensitivity comparable to nuclear medicine. To foster future applications in MPI, this new biomedical imaging field is welcoming researchers with expertise in imaging physics, magnetic nanoparticle synthesis and functionalization, nanoscale physics, and small animal imaging applications.

Introduction

Magnetic particle imaging (MPI) is a new tracer imaging technique first introduced by Philips, Hamburg[1]. MPI directly images the location and concentration of superparamagnetic iron oxide nanoparticle (SPIO) tracers with time-varying magnetic fields and has remarkably high sensitivity and contrast. Several SPIOs are clinically approved and currently on the market, including Feraheme (ferumoxytol), which is FDA approved for treatment of anemia in chronic kidney disease (CKD) patients[2]. Outside of the United States, SPIOs are available for patient imaging (Resovist), sentinel lymph node localization (Sienna) and hyperthermia (NanoTherm) applications[3–5]. Safe, radiation-free scanning in MPI combined with high-contrast, high-sensitivity imaging gives MPI fundamental advantages in vascular imaging and cell-tracking, which we discuss in this review.

[+] xizhou@berkeley.edu.

[*]Present Address: Magnetic Insight, Inc., Alameda, California 94501, United States

The physics of MPI relies on the electronic magnetization of SPIOs[1]. When an excitation field is applied to SPIOs in the field-of-view (FOV), the magnetic dipoles reorient rapidly in response. Much like in MRI, the change in magnetization can be visualized via Faraday's law with a receiver coil. Unlike MRI, the change is of electronic magnetization, rather than nuclear magnetization. This results in a higher sensitivity for MPI, as the electronic magnetization of iron is 22 million times stronger than that of the nuclear magnetization of water at 7 Tesla[6]. To localize this signal, a large gradient field is used. Outside of a small region with a close to zero field, termed the field free region (FFR), the gradient locks SPIOs in place even if the excitation field is applied. Inside the FFR, the SPIOs reorient in response to the excitation field. By rastering this FFR across each point in the FOV, an image is created.

MPI sensitivity can be as low as nanograms of iron (corresponding to as few as ~200 cells for cell tracking applications), and resolution can be as fine as ~1 mm[7,8]. These specifications were obtained on academic prototype scanners. Commercial preclinical MPI scanners were only recently introduced by Bruker GmbH and Magnetic Insight Inc, and specifications are steadily improving. Theoretical work predicts that a human MPI scanner could have picogram sensitivity in a 1 second scan[9] and technical improvements have been made approaching this goal[10]. MPI has no view limitations, and it works robustly even in the lungs and bones, where MRI and Ultrasound routinely fail. For instance, Fig. 3b clearly resolves SPIO-labeled stem cells in the lungs. Indeed, researchers have demonstrated proof-of-concept studies for MPI imaging of lung perfusion and ventilation[11–13]. MPI also has no depth limitations, unlike optical imaging methods. Many molecular reporters employed in cell culture studies and small animals employ optical fluorescence or bioluminescence probes, which are fundamentally limited by optical scattering and attenuation to surface applications. Last, unlike radiotracers, the SPIOs reporter "half life" is essentially infinite, enabling researchers to track the location of labeled cells even three months after introduction to a murine model[14]. This may be enabling since Nuclear Medicine reporters last for only hours (FDG 2 hours half life, Tc-99m 6 hours, In-111 2.8 days) while many pathophysiologic processes require weeks to manifest. Finally, MPI obtains a dose-limited sensitivity that is already competitive with Nuclear Medicine method on prototype MPI scanners.

In this review, we discuss recent applications in MPI, broadly divided into vascular imaging and cell tracking, as described in Fig. 1. Additionally, we discuss current needs in tracer development to enable future applications in MPI molecular imaging.

Vascular Imaging

The earliest applications of MPI focused on vascular imaging with untargeted SPIOs, such as 3D imaging of a beating mouse heart using Resovist[15]. This early work emphasized some of the inherent advantages of MPI – three-dimensional, high-contrast and fast imaging. Both imaging speed and circulation time of the MPI tracers is crucial for vascular applications.

SPIOs used in MPI typically have a hydrodynamic diameter between 50–100 nm, and they remain in the bloodstream until cleared by the reticuloendothelial system[16]. Circulation time

varies from minutes to hours depending on the nanoparticle coating. Early MPI researchers typically relied on ferucarbutran (also known as Resovist or VivoTrax), which is a cyclodextrin coated SPIO originally designed as a MRI liver imaging agent to highlight cancerous lesions[15]. It targets the liver within minutes[3]. The Krishnan group at University of Washington developed SPIOs with 2-fold better spatial resolution compared to Ferucarbutran and extended the circulation time of MPI SPIOs to 2+ hours in mice and 4+ hours in rats using polyethylene glycol coatings[17,18]. Alternative approaches to increasing MPI tracer circulation time include loading SPIOs into red blood cells[7,19,20]. These long-circulating tracers are crucial for applications like cancer imaging via the enhanced permeability and retention (EPR) effect[21••], brain imaging for traumatic brain injury (TBI) and stroke via visualizing cerebral blood volume and cerebral blood flow[22••,23], and gastrointestinal (GI) bleed imaging[24]. Each of these applications shown in Fig. 2 requires imaging over hours or days, and hence long circulating SPIO tracers offer MPI an advantage over nuclear medicine techniques, in which radionuclide decay limits the imaging time course. As an example, longer circulation time enables blood volume and blood perfusion studies in the brain, which could aid in stroke diagnosis and treatment planning. We can also appreciate the information available from the high resolution of MPI optimized tracers. For instance, in Fig. 2a at 10 minutes the initial wash-in of nanoparticles into the tumor margins is visible. This subtle rim enhancement is discernible hours before the SPIOs have highlighted the entire tumor at the 6 hour time point.

Recently, groups have employed both biochemical and biomechanical targeting moieties on SPIO surfaces to highlight pathophysiologies. Biochemical active targeting to cancers includes using lactoferrin to highlight brain glioma[25,26], while biomechanical targeting includes labeling macroaggregated albumin (MAA) with SPIOs to evaluate lung perfusion or directly administering nebulized SPIOs to the lung airways[11–13]. Unlike radiotracers, SPIO signal is stable over time, obviating the need for preparation immediately before patient use. The convenience and image quality of 3D MPI with targeted SPIOs will enable MPI scans as a compelling alternative to FDG-PET or Tc99m-V/Q scintigraphy for diagnosing cancer and pulmonary embolism, respectively. Future work in vascular imaging will continue in this vein to highlight specific pathophysiologies and harness the increasing resolution of MPI technology to highlight previously hidden perfusion behavior.

Cell Tracking

In recent years, stem cell tracking has gained research traction as a theranostic technique. Successful stem cell therapy requires verification that stem cells reach their intended destination, remain there over time and maintain viability to eventually create functional tissues or organs. MPI tracking of stem cells, shown in Fig. 3, has been demonstrated to quantitatively image the biodistribution and fate of intravenously administered stem cells in rats, neural implants of stem cells in rats, and neural implants of stem cells in mice[27•,14,28]. Of note is that the study tracking the biodistribution of intravenously administered stem cells was able to robustly image the presence of stem cells in the lungs, an area which is traditionally difficult for MRI and Ultrasound due to artifacts caused by air-tissue interfaces. Moreover, the neural implant work imaged stem cells over 87 days, a study which would not be possible with the clinical tracer modalities today due to the need for radioactively

decaying tracers. These early studies on stem cell lines have sparked further interest in the field of MPI stem cell tracking, leading to work demonstrating that MPI can be used to image pancreatic islet transplants in mice and work developing new nanoparticle agents for multimodal imaging of stem cells, including via MPI[29,30]. These studies demonstrated up to 200-cell sensitivity, which is far more sensitive than other medical imaging modalities[31]. Last, recent progress has been made in correlating MPI relaxation times to stem cell viability *in vivo*[32]. This technique relies on analyzing the harmonic spectra of the MPI signal (Magnetic Particle Spectroscopy - MPS) to determine if the SPIOs are still within the cell or have been released to the outside after cell death. With new particle and arbitrary excitation design[33], it may be possible to further distinguish stem-like states versus apoptotic or non-stem states.

Researchers have recently explored MPI for tracking prelabeled white blood cells (WBCs), which could emerge as a radiation-free alternative to infection imaging via traditional WBC-In111 scintigraphy (Gaudet *et al.*, Zhang *et al.*, Chandrasekharan *et al.*, World Molecular Imaging Conference, Philadelphia, September 2017). Preliminary work has shown that MPI can track cultured macrophages in both healthy and middle cerebral artery occlusion (MCAO) stroke mice, and tumor-associated macrophages in a 4T1 mouse model of metastatic cancer. Future work in MPI cell tracking is expected to extend these imaging studies to theranostic applications, such as tracking stem cell migration for disease treatment, or immune cell migration for immunotherapy treatment of cancers.

We note that the theranostic potential of MPI extends far beyond guiding cell-based treatments. Although this review focuses on MPI imaging applications, extensive work has also been performed demonstrating the utility of MPI for ionizing radiation-free surgical guidance[34–37] and therapeutic guidance, such as with magnetic hyperthermia[38–42].

Tracer Development

In the early days of MPI, researchers had to rely on SPIOs designed for T2* or T1-weighted MRI contrast agents[43]. Since MRI and MPI “see” SPIOs with completely different physics, the MPI performance of these SPIOs was not ideal. Dramatic improvements in sensitivity and image resolution have been enabled through tailoring of SPIOs to MPI’s unique physics[44–46]. Both theory and experiment have shown that 5–20 nm core sizes show poor resolution[47–49]. Larger core sizes (>27 nm) do not perform as well as the optimal range of 20–26 nm, due to relaxation blurring[50]. While 1–2 mm resolution is comparable to nuclear medicine’s resolution, a dramatic improvement in spatial resolution (100 microns) would obviate perhaps the last technical weakness of MPI. Since image resolution is improved both by either better SPIOs or higher scanner gradients, these MPI-tailored SPIOs could dramatically reduce scanner cost. A ten-fold improvement in SPIO magnetic resolution could reduce the cost of a clinical MPI scanner by nearly one-hundred-fold. Hence, high-resolution SPIOs remain an exciting and crucial area in MPI research to enable safe and cost-effective human MPI.

Beyond improving MPI signal and resolution, harnessing MPI physics to provide molecular contrast is an exciting research area. Color MPI extracts information about SPIO relaxation

to distinguish between nanoparticles with different relaxation dynamics and opens the door to multiplexing in MPI, similar to fluorescence multiplexing[51]. This work has recently been extended to *in vivo* imaging, as shown in Fig. 4 (Hensley *et al.*, World Molecular Imaging Conference, Philadelphia, September 2017). Relaxation mechanisms include Néel and Brownian, which are strongly influenced by the viscosity of the medium. In general, smaller particles exhibit mainly Néel behavior and are unaffected by the media viscosity or by binding. Larger particles exhibit mainly Brownian behavior and are very sensitive to media viscosity and to binding. Small relaxation changes can be detected via color MPI, but even standard MPI can detect large relaxation changes[52•]. MPI has seen only limited research into targeted nanoparticle coatings that target specific pathophysiologies[53•,54]. It will be exciting to see the vast area of nanomedicine research applied to MPI-targeted SPIOs for high specificity and sensitivity diagnosis of disease with zero ionizing radiation.

Conclusion

Magnetic particle imaging is an emerging SPIO tracer imaging modality with superb image sensitivity and zero tissue background signal, enabling unprecedented contrast-to-noise ratio (CNR) for a zero-radiation imaging modality. MPI uses no ionizing radiation and uses SPIO tracers, some of which have been used safely in patients. The MPI signal is the same anywhere and at any depth in the body, allowing for quantitative imaging, including in the lungs or bone marrow, which are challenging regions for MRI, Ultrasound and X-ray. Here, we focused on recent vascular perfusion imaging and cell tracking applications of MPI. Emerging applications include real-time guidance of surgery and magnetic hyperthermia. Color MPI could soon enable molecular contrast in MPI, distinguishing bound from unbound antibodies *in vivo*. Industry researchers are rapidly developing preclinical and, soon, clinical MPI scanners. MPI scanners may be integrated with MRI[55] or CT scanners, akin to hybrid PET-CT scanners. The high-contrast, ionizing radiation-free and superb sensitivity of MPI is expected to usher in new applications for preclinical and clinical researchers.

Acknowledgements

We are grateful for funding support from NSF-GRFP. Additionally, we would like to thank Caylin VanHook for help with designing the graphical abstract.

References

1. Gleich B and Weizenecker J (2005). Tomographic imaging using the nonlinear response of magnetic particles. Nature 435, 1214–1217. [PubMed: 15988521]
2. Lu M, Cohen MH, Rieves D, and Pazdur R (2010). FDA report: Ferumoxytol for intravenous iron therapy in adult patients with chronic kidney disease. Am. J. Hematol 85, 315–319. [PubMed: 20201089]
3. Reimer P and Balzer T (2003). Ferucarbotran (Resovist): a new clinically approved RES-specific contrast agent for contrast-enhanced MRI of the liver: properties, clinical development, and applications. Eur. Radiol 13, 1266–1276. [PubMed: 12764641]
4. Thill M, Kurylcio A, Welter R, van Haasteren V, Grosse B, Berclaz G, Polkowski W, and Hauser N (2014). The Central-European SentiMag study: sentinel lymph node biopsy with superparamagnetic iron oxide (SPIO) vs. radioisotope. Breast 23, 175–179. [PubMed: 24484967]

5. Weissig V, Pettinger TK, and Murdock N (2014). Nanopharmaceuticals (part 1): products on the market. Int. J. Nanomedicine 9, 4357–4373. [PubMed: 25258527]

6. Saritas EU, Goodwill PW, Croft LR, Konkle JJ, Lu K, Zheng B, and Conolly SM (2013). Magnetic particle imaging (MPI) for NMR and MRI researchers. J. Magn. Reson 229, 116–126. [PubMed: 23305842]

7. Rahmer J, Antonelli A, Sfara C, Tiemann B, Gleich B, Magnani M, Weizenecker J, and Borgert J (2013). Nanoparticle encapsulation in red blood cells enables blood-pool magnetic particle imaging hours after injection. Phys. Med. Biol 58, 3965–3977. [PubMed: 23685712]

8. Panagiotopoulos N, Duschka RL, Ahlborg M, Bringout G, Debbeler C, Graeser M, Kaethner C, Ludtke-Buzug K, Medimagh H, Stelzner J, et al. (2015). Magnetic particle imaging: current developments and future directions. Int. J. Nanomedicine 10, 3097–3114. [PubMed: 25960650]

9. Gleich B (2014). Principles and Applications of Magnetic Particle Imaging (Wiesbaden: Springer Fachmedien Wiesbaden).

10. Graeser M, Knopp T, Szwargulski P, Friedrich T, von Gladiss A, Kaul M, Krishnan KM, Ittrich H, Adam G, and Buzug TM (2017). Towards Picogram Detection of Superparamagnetic Iron-Oxide Particles Using a Gradiometric Receive Coil. Sci. Rep 7, 6872. [PubMed: 28761103]

11. Zhou XY, Jeffris KE, Yu EY, Zheng B, Goodwill PW, Nahid P, and Conolly SM (2017). First in vivo magnetic particle imaging of lung perfusion in rats. Phys. Med. Biol 62, 3510–3522. [PubMed: 28218614]

12. Banura N and Murase K (2017). Magnetic particle imaging for aerosol-based magnetic targeting. Jpn. J. Appl. Phys 56, 088001.

13. Nishimoto K, Mimura A, Aoki M, Banura N, and Murase K (2015). Application of Magnetic Particle Imaging to Pulmonary Imaging Using Nebulized Magnetic Nanoparticles. OJMI 05, 49–55.

14. Zheng B, Vazin T, Goodwill PW, Conway A, Verma A, Saritas EU, Schaffer D, and Conolly SM (2015). Magnetic Particle Imaging tracks the long-term fate of in vivo neural cell implants with high image contrast. Sci. Rep 5, 14055. [PubMed: 26358296]

15. Weizenecker J, Gleich B, Rahmer J, Dahnke H, and Borgert J (2009). Three-dimensional real-time in vivo magnetic particle imaging. Phys. Med. Biol 54, L1–L10. [PubMed: 19204385]

16. Gupta AK and Gupta M (2005). Synthesis and surface engineering of iron oxide nanoparticles for biomedical applications. Biomaterials 26, 3995–4021. [PubMed: 15626447]

17. Khandhar AP, Ferguson RM, Arami H, and Krishnan KM (2013). Monodisperse magnetite nanoparticle tracers for in vivo magnetic particle imaging. Biomaterials 34, 3837–3845. [PubMed: 23434348]

18. Keselman P, Yu E, Zhou X, Goodwill P, Chandrasekharan P, Ferguson RM, Khandhar A, Kemp S, Krishnan K, Zheng B, et al. (2017). Tracking short-term biodistribution and long-term clearance of SPIO tracers in magnetic particle imaging. Phys. Med. Biol 62, 3440. [PubMed: 28177301]

19. Markov DE, Boeve H, Gleich B, Borgert J, Antonelli A, Sfara C, and Magnani M (2010). Human erythrocytes as nanoparticle carriers for magnetic particle imaging. Phys. Med. Biol 55, 6461–6473. [PubMed: 20959685]

20. Takeuchi Y, Suzuki H, Sasahara H, Ueda J, Yabata I, Itagaki K, Saito S, and Murase K (2014). Encapsulation of Iron Oxide Nanoparticles into Red Blood Cells as a Potential Contrast Agent for Magnetic Particle Imaging. Advanced Biomedical Engineering 3, 37–43.

21••. Yu EY, Bishop M, Zheng B, Ferguson RM, Khandhar AP, Kemp SJ, Krishnan KM, Goodwill PW, and Conolly SM (2017). Magnetic Particle Imaging: A Novel in Vivo Imaging Platform for Cancer Detection. Nano Lett. 17, 1648–1654. [PubMed: 28206771] ••First cancer imaging using MPI. Long-circulating, high-resolution MPI tracers allow observation of tumor wash-in and wash-out dynamics over several hours.

22••. Ludewig P, Gdaniec N, Sedlacik J, Forkert ND, Szwargulski P, Graeser M, Adam G, Kaul MG, Krishnan KM, Ferguson RM, et al. (2017). Magnetic Particle Imaging for Real-Time Perfusion Imaging in Acute Stroke. ACS Nano 11, 10480–10488. [PubMed: 28976180] ••First imaging of stroke using MPI. 47 fps imaging speed allows fast and accurate assessment of cerebral perfusion.

23. Orendorff R, Peck AJ, Zheng B, Shirazi SN, Matthew Ferguson R, Khandhar AP, Kemp SJ, Goodwill P, Krishnan KM, Brooks GA, et al. (2017). First in vivo traumatic brain injury imaging via magnetic particle imaging. Phys. Med. Biol 62, 3501–3509. [PubMed: 28378708]
24. Yu EY, Chandrasekharan P, Berzon R, Tay ZW, Zhou XY, Khandhar AP, Ferguson RM, Kemp SJ, Zheng B, Goodwill PW, et al. (2017). Magnetic Particle Imaging for Highly Sensitive, Quantitative, and Safe in Vivo Gut Bleed Detection in a Murine Model. ACS Nano 11, 12067–12076.
25. Arami H, Teeman E, Troksa A, Bradshaw H, Saatchi K, Tomitaka A, Gambhir SS, Häfeli UO, Liggitt D, and Krishnan KM (2017). Tomographic magnetic particle imaging of cancer targeted nanoparticles. Nanoscale 9, 18723–18730. [PubMed: 29165498]
26. Tomitaka A, Arami H, Gandhi S, and Krishnan KM (2015). Lactoferrin conjugated iron oxide nanoparticles for targeting brain glioma cells in magnetic particle imaging. Nanoscale 7, 16890–16898. [PubMed: 26412614]
27•. Zheng B, von See MP, Yu E, Gunel B, Lu K, Vazin T, Schaffer DV, Goodwill PW, and Conolly SM (2016). Quantitative Magnetic Particle Imaging Monitors the Transplantation, Biodistribution, and Clearance of Stem Cells In Vivo. Theranostics 6, 291–301. [PubMed: 26909106] •Evaluation of the clearance of administered stem cells from lungs to liver and spleen via MPI showed feasibility for MPI cell tracking throughout the entire body.
28. Bulte JWM, Walczak P, Janowski M, Krishnan KM, Arami H, Halkola A, Gleich B, and Rahmer J (2015). Quantitative “Hot Spot” Imaging of Transplanted Stem Cells using Superparamagnetic Tracers and Magnetic Particle Imaging (MPI). Tomography 1, 91–97. [PubMed: 26740972]
29. Wang P, Goodwill PW, Pandit P, Gaudet J, Ross A, Wang J, Yu E, Hensley DW, Doyle TC, Contag CH, et al. (2018). Magnetic particle imaging of islet transplantation in the liver and under the kidney capsule in mouse models. Quant. Imaging Med. Surg 8, 114–122. [PubMed: 29675353]
30. Lemaster JE, Chen F, Kim T, Hariri A, and Jokerst JV (2018). Development of a Trimodal Contrast Agent for Acoustic and Magnetic Particle Imaging of Stem Cells. ACS Appl. Nano Mater 1, 1321–1331.
31. Nguyen PK, Riegler J, and Wu JC (2014). Stem cell imaging: from bench to bedside. Cell Stem Cell 14, 431–444. [PubMed: 24702995]
32. Fidler F, Steinke M, Kraupner A, Gruttner C, Hiller KH, Briel A, Westphal F, Walles H, and Jakob PM (2015). Stem Cell Vitality Assessment Using Magnetic Particle Spectroscopy. IEEE Trans. Magn 51, 1–4. [PubMed: 26203196]
33. Tay ZW, Goodwill PW, Hensley DW, Taylor LA, Zheng B, and Conolly SM (2016). A High-Throughput, Arbitrary-Waveform, MPI Spectrometer and Relaxometer for Comprehensive Magnetic Particle Optimization and Characterization. Sci. Rep 6, 34180. [PubMed: 27686629]
34. Salamon J, Hofmann M, Jung C, Kaul MG, Werner F, Them K, Reimer R, Nielsen P, Vom Scheidt A, Adam G, et al. (2016). Magnetic Particle / Magnetic Resonance Imaging: In-Vitro MPI-Guided Real Time Catheter Tracking and 4D Angioplasty Using a Road Map and Blood Pool Tracer Approach. PLoS One 11, e0156899. [PubMed: 27249022]
35. Haegele J, Rahmer J, Gleich B, Borgert J, Wojtczyk H, Panagiotopoulos N, Buzug TM, Barkhausen J, and Vogt FM (2012). Magnetic particle imaging: visualization of instruments for cardiovascular intervention. Radiology 265, 933–938. [PubMed: 22996744]
36. Rahmer J, Wirtz D, Bontus C, Borgert J, and Gleich B (2017). Interactive Magnetic Catheter Steering With 3-D Real-Time Feedback Using Multi-Color Magnetic Particle Imaging. IEEE Trans. Med. Imaging 36, 1449–1456. [PubMed: 28287965]
37. Duschka RL, Wojtczyk H, Panagiotopoulos N, Haegele J, Bringout G, Buzug TM, Barkhausen J, and Vogt FM (2014). Safety measurements for heating of instruments for car-diovascular interventions in magnetic particle imaging (MPI) - first experiences. J. Healthc. Eng 5, 79–93. [PubMed: 24691388]
38. Kobayashi S, Ohki A, Tanoue M, Inaoka Y, and Murase K (2017). Comparative Study of Extracellular and Intracellular Magnetic Hyperthermia Treatments Using Magnetic Particle Imaging. Open Journal of Applied Sciences 7, 647.

39. Hensley D, Tay ZW, Dhavalikar R, Zheng B, Goodwill P, Rinaldi C, and Conolly S (2017). Combining magnetic particle imaging and magnetic fluid hyperthermia in a theranostic platform. Phys. Med. Biol 62, 3483–3500. [PubMed: 28032621]
40. Kuboyabu T, Yabata I, Aoki M, Banura N, Nishimoto K, Mimura A, and Murase K (2016). Magnetic Particle Imaging for Magnetic Hyperthermia Treatment: Visualization and Quantification of the Intratumoral Distribution and Temporal Change of Magnetic Nanoparticles in Vivo. OJMI 06, 1–15.
41. Kuboyabu T, Yamawaki M, Aoki M, Ohki A, and Murase K (2016). Quantitative Evaluation of Tumor Early Response to Magnetic Hyperthermia combined with Vascular Disrupting Therapy using Magnetic Particle Imaging. Int J Nanomed Nanosurg 2, 1–7.
42. Tay ZW, Chandrasekharan P, Chiu-Lam A, Hensley DW, Dhavalikar R, Zhou XY, Yu EY, Goodwill PW, Zheng B, Rinaldi C, et al. (2018). Magnetic Particle Imaging-Guided Heating in Vivo Using Gradient Fields for Arbitrary Localization of Magnetic Hyperthermia Therapy. ACS Nano Article ASAP.
43. Wang YXJ (2011). Superparamagnetic iron oxide based MRI contrast agents: Current status of clinical application. Quant. Imaging Med. Surg 1, 35–40. [PubMed: 23256052]
44. Eberbeck D, Dennis CL, Huls NF, Krycka KL, Gruttner C, and Westphal F (2013). Multicore Magnetic Nanoparticles for Magnetic Particle Imaging. IEEE Trans. Magn 49, 269–274.
45. Ferguson RM, Khandhar AP, and Krishnan KM (2012). Tracer design for magnetic particle imaging (invited). J. Appl. Phys 111, 07B318.
46. Ferguson RM, Khandhar AP, Kemp SJ, Arami H, Saritas EU, Croft LR, Konkle J, Goodwill PW, Halkola A, Rahmer J, et al. (2015). Magnetic particle imaging with tailored iron oxide nanoparticle tracers. IEEE Trans. Med. Imaging 34, 1077–1084. [PubMed: 25438306]
47. Arami H, Ferguson RM, Khandhar AP, and Krishnan KM (2013). Size-dependent ferrohydrodynamic relaxometry of magnetic particle imaging tracers in different environments. Med. Phys 40, 071904. [PubMed: 23822441]
48. Goodwill PW and Conolly SM (2010). The X-space formulation of the magnetic particle imaging process: 1-D signal, resolution, bandwidth, SNR, SAR, and magnetostimulation. IEEE Trans. Med. Imaging 29, 1851–1859. [PubMed: 20529726]
49. Rahmer J, Weizenecker J, Gleich B, and Borgert J (2009). Signal encoding in magnetic particle imaging: properties of the system function. BMC Med. Imaging 9, 4. [PubMed: 19335923]
50. Tay ZW, Hensley DW, Vreeland EC, Zheng B, and Conolly SM (2017). The relaxation wall: experimental limits to improving MPI spatial resolution by increasing nanoparticle core size. Biomed. Phys. Eng. Express 3, 035003. [PubMed: 29250434]
51. Rahmer J, Halkola A, Gleich B, Schmale I, and Borgert J (2015). First experimental evidence of the feasibility of multi-color magnetic particle imaging. Phys. Med. Biol 60, 1775–1791. [PubMed: 25658130]
52•. Gandhi S, Arami H, and Krishnan KM (2016). Detection of Cancer-Specific Proteases Using Magnetic Relaxation of Peptide-Conjugated Nanoparticles in Biological Environment. Nano Lett. 16, 3668–3674. [PubMed: 27219521] • Authors designed and fabricated a nanoparticle system that changes magnetic relaxation in response to cancer-specific proteases.
53•. Song G, Chen M, Zhang Y, Cui L, Qu H, Zheng X, Wintermark M, Liu Z, and Rao J (2018). Janus Iron Oxides @ Semiconducting Polymer Nanoparticle Tracer for Cell Tracking by Magnetic Particle Imaging. Nano Lett. 18, 182–189. [PubMed: 29232142] •Recent work on SPIO development highlights the utility of tailored MPI tracers for higher sensitivity and multimodal imaging.
54. Tomitaka A, Arami H, Huang Z, Raymond A, Rodriguez E, Cai Y, Febo M, Takemura Y, and Nair M (2017). Hybrid magneto-plasmonic liposomes for multimodal image-guided and brain-targeted HIV treatment. Nanoscale 10, 184–194. [PubMed: 29210401]
55. Franke J, Heinen U, Lehr H, Weber A, Jaspard F, Ruhm W, Heidenreich M, and Schulz V (2016). System Characterization of a Highly Integrated Preclinical Hybrid MPI-MRI Scanner. IEEE Trans. Med. Imaging 35, 1993–2004. [PubMed: 26991821]

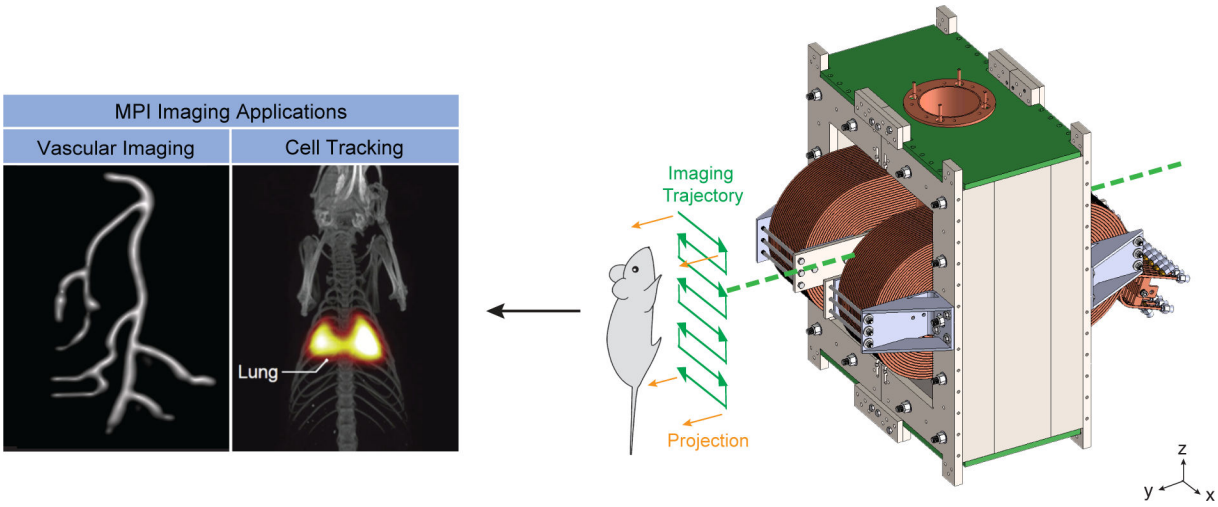

Figure 1. MPI Imaging Applications today.

Broadly, MPI researchers have pursued vascular imaging and cell tracking. In vascular imaging, researchers have used both tracers that passively highlight the physiology of interest, or are specifically targeted via an antibody or other moiety. In cell tracking, researchers have imaged several types of stem cells, and more recently interest has grown in imaging immune cells for infection imaging, immunotherapy tracking and early-stage cancer detection. Scanner schematic adapted with permission from[24]. Copyright 2017 American Chemical Society. Vascular imaging phantom image courtesy of Justin Konkle. Stem cell tracking image courtesy of Bo Zheng. Image fusion of MPI (color) and CT (grey).

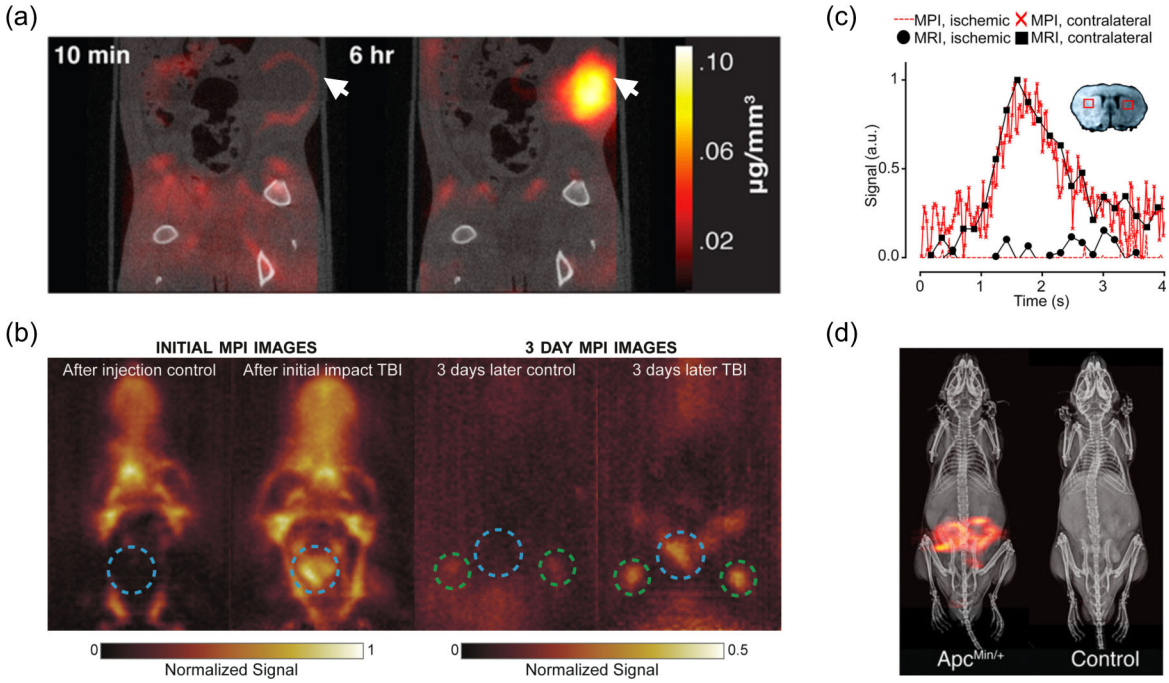

Figure 2. Selected MPI vascular imaging applications.

(a) Cancer imaging of rats. MPI/CT of a human breast tumor xenograft shows enhanced image contrast 6 h after SPIO injection. Arrows indicate tumor volume. Adapted with permission from[21••]. Copyright 2017 American Chemical Society. *(b) Traumatic brain injury (TBI) imaging of rats*. Blue dotted circle indicates impact site. Green circles indicate lymph nodes. The TBI rat has significant signal from the hemorrhage, as well as signal inside the lymph nodes, unlike the control[23]. Copyright Institute of Physics and Engineering in Medicine. Adapted with permission of IOP Publishing. All rights reserved. *(c) Stroke imaging of mice*. MRI and MPI signals were plotted over time for certain selected regions of interest: filled black circles, MRI signal ischemic hemisphere; filled black squares, MRI signal healthy hemisphere; red dotted line, MPI signal ischemic hemisphere; red crosses, MPI signal healthy hemisphere). The concentration–time curves of the MPI and MRI showed similar progression and reduced wash-out of the contrast agents into the ischemic hemisphere. Reprinted with permission from[22••]. Copyright 2017 American Chemical Society. *(d) GI bleed imaging of mice*. Dynamic projection MPI and subtraction MPI images, both co-registered to X-ray anatomical reference, allow detection and quantification of GI bleed in a ApcMin/+ mouse model predisposed to GI polyp development. Reprinted with permission from[24]. Copyright 2017 American Chemical Society.

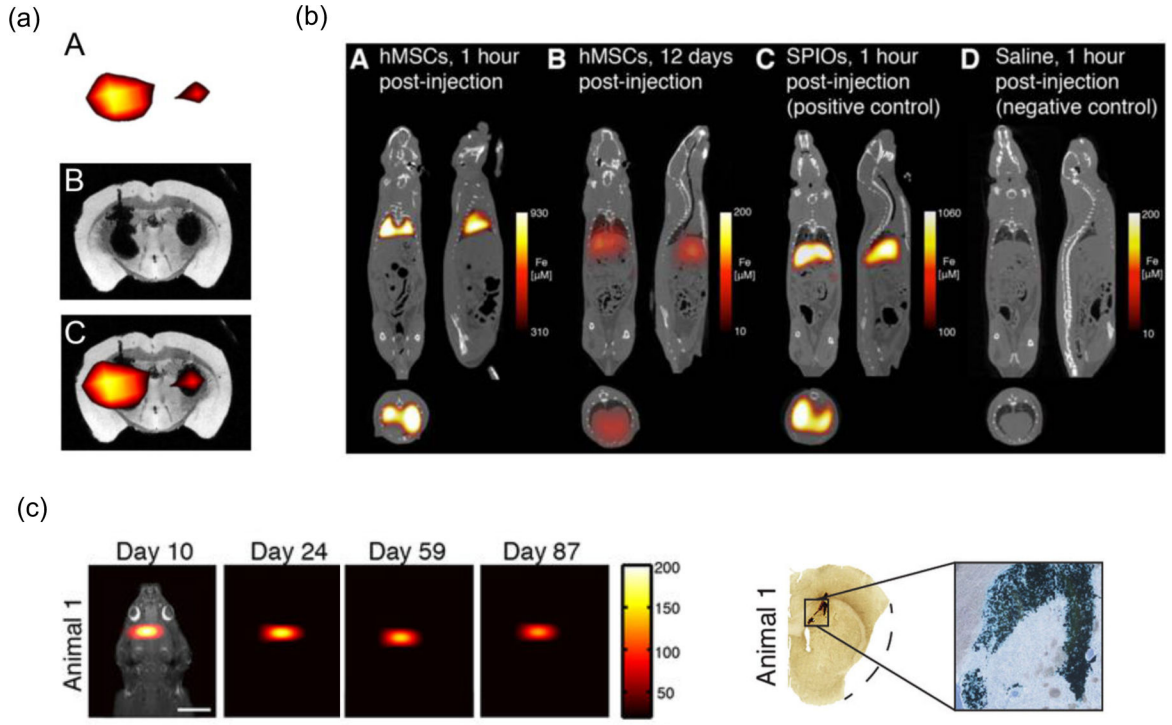

Figure 3. Selected MPI cell tracking applications.

(a) Stem cell implant imaging in mice. MPI (A), MRI (B) and corresponding overlay MPI/MRI (C) of a mouse brain transplanted with 1×10^5 (left hemisphere) or 5×10^4 (right hemisphere) SPIO-labeled mesenchymal stem cells. Reproduced from[28] under the CC BY-NC-ND license (http://creativecommons.org/licenses/by-nc-nd/4.0/). *b) Stem cell injection imaging in rats. 3D MPI-CT imaging of intravenously injected human mesenchymal stem cells (hMSCs) and SPIO control*. (A) MPI imaging of hMSC tail vein injections <1 hr post-injection shows substantial hMSC localization to lung. (B) At 12 days, hMSC tail vein injections show significant total clearance and liver migration. (C) MPI imaging of SPIO-only tail vein injections less than one hour post-injection shows immediate uptake in liver and spleen. (D) Control injections of isotonic saline show no detectable MPI signal. Reproduced with permission from[27•] under the Creative Commons Attribution (CC BY-NC) License (https://creativecommons.org/licenses/by-nc/4.0/). *(c) Long-term stem cell implant imaging in rats*. (LEFT) Longitudinal MPI imaging of 5×10^5 SPIO-labeled human NPCs implanted in the forebrain cortex over 87 days. Scale bar 1 cm. Color intensity in *ng/mm*^{2}. (RIGHT) Postmortem Prussian blue (PB) staining confirms presence of iron-labeled cells at administration site. Adapted with permission from[27•] under the Creative Commons CC BY License (https://creativecommons.org/licenses/by/4.0/).

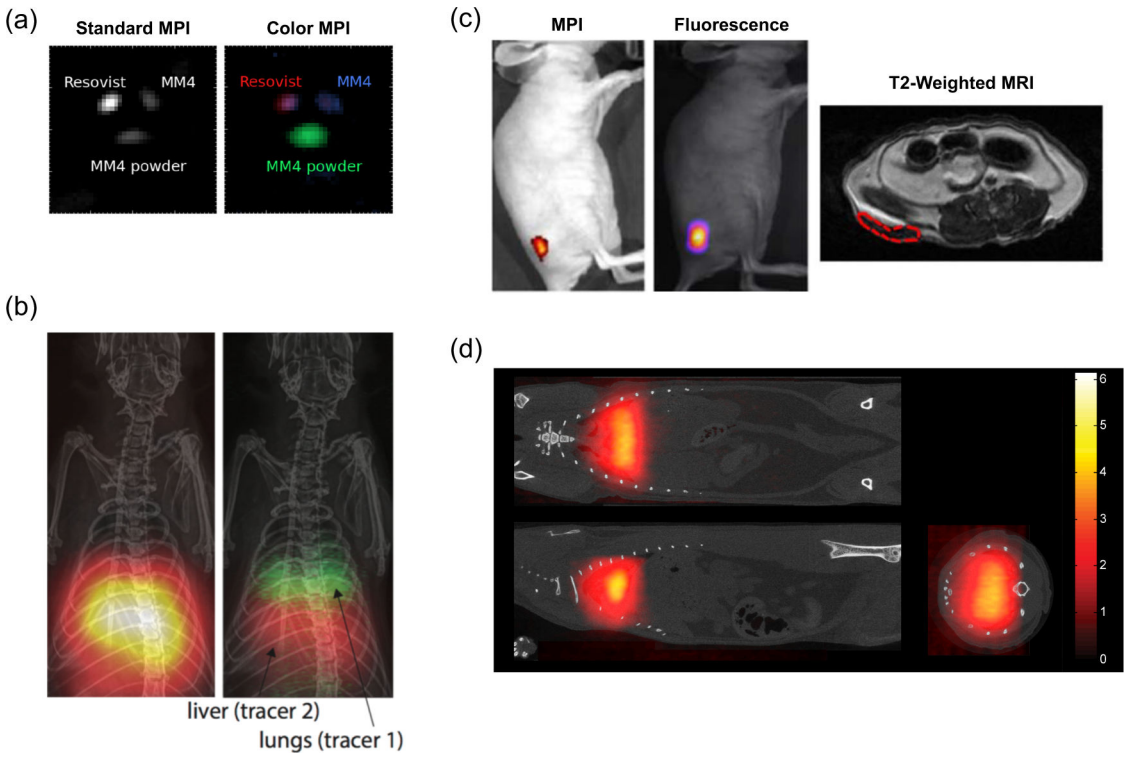

Figure 4. Recent progress in tracer technologies.

(a) In vitro tri-color MPI. Three different MPI tracers are indistinguishable in a standard MPI reconstruction algorithm, but can be distinguished after applying a multi-color reconstruction algorithm. Adapted with permission from[51] under the Creative Commons Attribution 3.0 license (http://creativecommons.org/licenses/by/3.0). *(b) In vivo dual-color MPI.* Rat lung and liver are targeted with two nanoparticles with different relaxation behavior. In standard MPI, the organs are indistinguishable, but after the colorizing algorithm the organs can be distinguished based on the relaxation behavior of the SPIOs within. Image courtesy of Daniel Hensley. *(c) Multi-modal Janus iron oxide MPI tracers.* SPIO tracers can be designed for multi-modality imaging. Mice were subcutaneously implanted with nanoparticle-labeled cells and imaged under MPI, fluorescence and T2-weighted MRI. Adapted with permission from[53•]. Copyright 2017 American Chemical Society. *(d) Lung perfusion imaging with MAA-SPIO.* Large macroaggregated albumin conjugated to SPIOs are biomechanically trapped in the rat lung, allowing imaging of blood perfusion through the lungs[11]. Institute of Physics and Engineering in Medicine. Adapted with permission of IOP Publishing. All rights reserved.